*Available online at* www.derpharmachemica.com

ISSN 0975-413X
CODEN (USA): PCHHAX

**Der Pharma Chemica, 2016, 8(4):329-337**
*(http://derpharmachemica.com/archive.html)*

# A DFT study of the inhibition of human phosphodiesterases PDE3A and PDE3B by a group of 2-(4-(1*H*-tetrazol-5-yl)-1*H*-pyrazol-1-yl)-4-(4-phenyl)thiazole derivatives

**Juan S. Gómez-Jeria* and Patricio Cornejo-Martínez**

*Quantum Pharmacology Unit, Department of Chemistry, Faculty of Sciences, University of Chile. Las Palmeras 3425, Santiago 7800003, Chile*

---

**ABSTRACT**

*Here we present the results of the investigation of the relationships between electronic structure and human phosphodiesterases PDE3A and PDE3B inhibition by a group of 2-(4-(1H-tetrazol-5-yl)-1H-pyrazol-1-yl)-4-(4-phenyl)thiazole derivatives. The electronic structure was obtained with Density Functional Theory at the B3LYP/6-31G(d,p) level after full geometry optimization. Statistically significant equations were obtained for both systems. Both inhibitory processes are orbital-controlled. The associated pharmacophores may provide information for possible modifications of the common skeleton.*

**Keywords**: Phosphodiesterases, PDE3A, PDE3B, DFT, QSAR, KPG method.

---

## INTRODUCTION

As another example destined to show that the Klopman-Peradejordi-Gómez (KPG) method is able to produce useful information about the relationships between electronic structure and several kinds of biological activities, we have focused our attention of the inhibition of phosphodiesterases (PDE). Phosphodiesterases are enzymes that breaks a phosphodiester bond. Among the many families of phosphodiesterases we are interested in cyclic nucleotide PDEs. The cyclic nucleotide PDEs catalyze the hydrolysis of cyclic AMP and cyclic GMP (cGMP), regulating the localization, duration, and amplitude of cyclic nucleotide signaling within subcellular domains. PDEs are thus significant regulators of signal transduction mediated by the abovementioned messenger molecules [1-27]. The PDE3 family in mammals comprises two members, PDE3A and PDE3B. The PDE3 isoforms are structurally analogous, containing an N-terminal domain and a C-terminus end. The 44-amino acid insertion in the catalytic domain varies in the PDE3 isoforms, and the N-terminal portions of the isoforms are rather divergent. PDE3A and PDE3B have strikingly analogous pharmacological and kinetic properties, but the difference is in the expression profiles and the affinity for cGMP. Presently, a small number of PDE inhibitors are employed for treating the pathophysiological dysregulation of cyclic nucleotide signaling in some disorders, including acute refractory cardiac failure, chronic obstructive pulmonary disease, erectile dysfunction, intermittent claudication and pulmonary hypertension. Several molecules and families of molecules have been synthesized and tested for the inhibition of different PDEs [5, 28-51].

In this paper we present the results the results of the application of the KPG method to the inhibition of phosphodiesterases PDE3A and PDE3B by a group of 2-(4-(1*H*-tetrazol-5-yl)-1*H*-pyrazol-1-yl)-4-(4-phenyl)thiazole derivatives.

## MATERIALS AND METHODS [52]

### The method [52].

The results presented here are obtained from what is now a routinary procedure. For this reason, we employ here a general model for the paper's structure. This model contains *standard* phrases for the presentation of the methods, calculations and results because they do not need to be rewritten repetitively. The method has been fully presented in earlier publications [53-58]. Therefore, we shall discuss only the results obtained in this study. The results of the successful application of the KPG method can be found elsewhere ([59-63] and references therein).

### Selection of molecules and biological activities.

The chosen molecules are a group of 2-(4-(1*H*-tetrazol-5-yl)-1*H*-pyrazol-1-yl)-4-(4-phenyl)thiazole and were selected from a recent study [29]. Their general formula and biological activity are displayed, respectively, in Fig. 1 and Table 1. The biological activity analyzed corresponds to the PDE3 (types A and B) inhibitory activities.

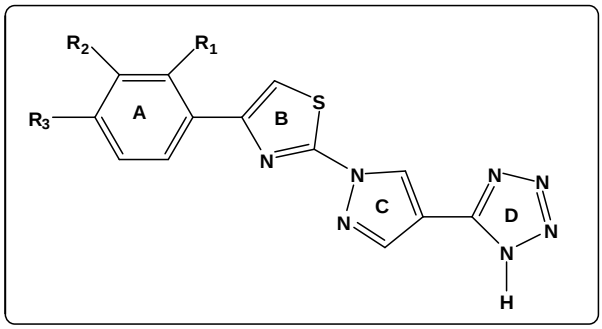


**Figure 1. General formula of 2-(4-(1*H*-tetrazol-5-yl)-1*H*-pyrazol-1-yl)-4-(4-phenyl) thiazole derivatives**

**Table 1. 2-(4-(1*H*-tetrazol-5-yl)-1*H*-pyrazol-1-yl)-4-(4-phenyl)thiazole derivatives and inhibitory activities**

| Mol. | $R_1$ | $R_2$ | $R_3$ | $\log(IC_{50})$ PDE3A | $\log(IC_{50})$ PDE3B |
|---|---|---|---|---|---|
| 1 | H | H | Cl | 0.39 | 0.58 |
| 2 | H | Cl | H | 0.48 | 0.70 |
| 3 | Cl | H | H | 0.56 | 0.77 |
| 4 | H | H | F | -0.62 | 0.37 |
| 5 | H | F | H | 0.16 | 0.67 |
| 6 | F | H | H | 0.28 | 0.67 |
| 7 | H | H | $NO_2$ | 0.79 | 0.86 |
| 8 | H | $NO_2$ | H | 0.84 | 0.93 |
| 9 | $NO_2$ | H | H | 0.87 | 1.01 |
| 10 | H | H | Me | 0.91 | 1.22 |
| 11 | H | Me | H | 0.96 | 1.16 |
| 12 | Me | H | H | 1.00 | 1.22 |
| 13 | H | H | OMe | 1.13 | 1.41 |
| 14 | H | OMe | H | 1.17 | 1.40 |
| 15 | OMe | H | H | 1.22 | 1.45 |

### Calculations.

The electronic structure of all molecules was calculated within the Density Functional Theory (DFT) at the B3LYP/6-31g(d,p) level after full geometry optimization. The Gaussian suite of programs was used [64]. All the information needed to calculate numerical values for the local atomic reactivity indices was obtained from the Gaussian results with the D-Cent-QSAR software [65]. All the electron populations smaller than or equal to 0.01 e were considered as zero [57]. Negative electron populations coming from Mulliken Population Analysis were corrected as usual [66]. Since the resolution of the system of linear equations is not possible because we have not enough molecules, we made use of Linear Multiple Regression Analysis (LMRA) techniques to find the best

solution. For each case, a matrix containing the dependent variable (the biological activity of each case) and the local atomic reactivity indices of all atoms of the common skeleton as independent variables was built. The Statistica software was used for LMRA [67].

We worked with the *common skeleton hypothesis* stating that there is a definite collection of atoms, common to all molecules analyzed, that accounts for nearly all the biological activity. The action of the substituents consists in modifying the electronic structure of the common skeleton and influencing the right alignment of the drug throughout the orientational parameters. It is hypothesized that different parts or this common skeleton accounts for almost all the interactions leading to the expression of a given biological activity. The common skeleton is shown in Fig. 2.

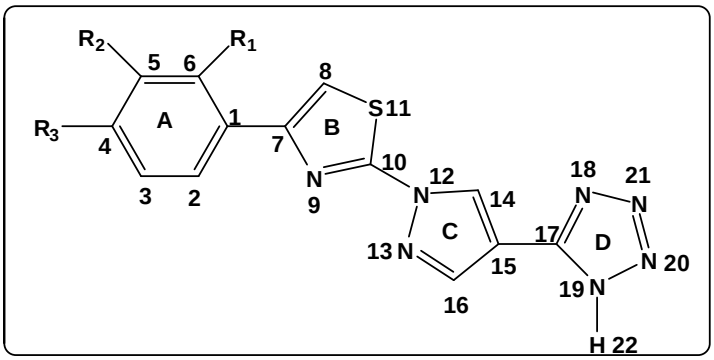


**Figure 2. Common skeleton of 2-(4-(1*H*-tetrazol-5-yl)-1*H*-pyrazol-1-yl)-4-(4-phenyl) thiazole derivatives**

## RESULTS

**Results for PDE3A inhibition.**

The best equation obtained was:

$$\log(IC_{50}) = 2.15 - 2.68F_{10}(LUMO+2)^* - 0.76F_{11}(LUMO+2)^* - \\ -7.04F_{11}(HOMO)^* + 0.41F_5(LUMO+2)^* \quad (1)$$

with n=14, R=0.99, $R^2$=0.99, adj-$R^2$=0.98, F(4,9)=166.03 ($p$<0.000001) and SD=0.07. No outliers were detected and no residuals fall outside the ±2σ limits. Here, $F_{10}(LUMO+2)^*$ is the Fukui index of the third lowest vacant MO localized on atom 10, $F_{11}(LUMO+2)^*$ is the Fukui index of the third lowest vacant MO localized on atom 11, $F_{11}(HOMO)^*$ is the Fukui index of the highest occupied MO localized on atom 11 and $F_5(LUMO+2)^*$ is the Fukui index of the third lowest vacant MO localized on atom 5. Tables 2 and 3 show the beta coefficients, the results of the t-test for significance of coefficients and the matrix of squared correlation coefficients for the variables of Eq. 1. There are no significant internal correlations between independent variables (Table 3). Figure 3 displays the plot of observed *vs.* calculated log($IC_{50}$).

**Table 2. Beta coefficients and t-test for significance of coefficients in Eq. 1**

| Var. | Beta | t(9) | p-level |
|---|---|---|---|
| $F_{10}(LUMO+2)^*$ | -0.49 | -10.86 | <0.000002 |
| $F_{11}(LUMO+2)^*$ | -0.54 | -12.63 | <0.000001 |
| $F_{11}(HOMO)^*$ | -0.36 | -8.55 | <0.00001 |
| $F_5(LUMO+2)^*$ | 0.14 | 3.18 | <0.01 |

**Table 3. Matrix of squared correlation coefficients for the variables in Eq. 1**

| | $F_{10}(LUMO+2)^*$ | $F_{11}(LUMO+2)^*$ | $F_{11}(HOMO)^*$ |
|---|---|---|---|
| $F_{11}(LUMO+2)^*$ | 0.12 | 1.00 | |
| $F_{11}(HOMO)^*$ | 0.07 | 0.02 | 1.00 |
| $F_5(LUMO+2)^*$ | 0.04 | 0.04 | 0.05 |

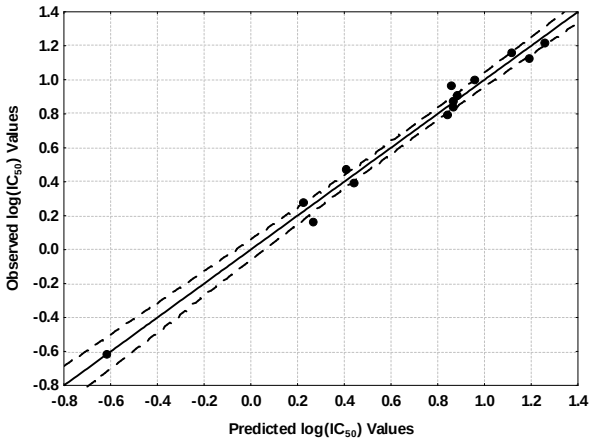


**Figure 3. Plot of predicted *vs*. observed log($IC_{50}$) values (Eq. 1). Dashed lines denote the 95% confidence interval**

The associated statistical parameters of Eq. 1 indicate that this equation is statistically significant and that the variation of the numerical values of a group of four local atomic reactivity indices of atoms of the common skeleton explains about 98% of the variation of log($IC_{50}$). Figure 3, spanning about 2.2 orders of magnitude, shows that there is a good correlation of observed *versus* calculated values and that almost all points are inside the 95% confidence interval. This can be considered as an indirect evidence that the common skeleton hypothesis works relatively well for this set of molecules. Note that when a local atomic reactivity index of an inner occupied MO (i.e., HOMO-1 and/or HOMO-2) or of a higher vacant MO (LUMO+1 and/or LUMO+2) appears in any equation, this means that the remaining of the upper occupied MOs (for example, if HOMO-2 appears, upper means HOMO-1 and HOMO) or the remaining of the empty MOs (for example, if LUMO+1 appears, lower means the LUMO) contribute to the interaction. Their absence in the equation only means that the variation of their numerical values does not account for the variation of the numerical value of the biological property.

**Results for PDE3B inhibition.**
The best equation obtained was:

$$\log(IC_{50}) = 0.53 - 0.11S_4^N(LUMO)^* - 0.11S_{18}^E(HOMO-2)^* \quad (2)$$

with n=15, R=0.96, $R^2$=0.91, adj-$R^2$=0.90, F(2,12)=64.20 ($p$<0.000001) and SD=0.11. No outliers were detected and no residuals fall outside the ±2σ limits. Here, $S_4^N(LUMO)^*$ is the nucleophilic superdelocalizability of the lowest vacant MO localized on atom 4 and $S_{18}^E(HOMO-2)^*$ is the electrophilic superdelocalizability of the third highest occupied MO localized on atom 18. Tables 4 and 5 show the beta coefficients, the results of the t-test for significance of coefficients and the matrix of squared correlation coefficients for the variables of Eq. 2. There are no significant internal correlations between independent variables (Table 5). Figure 4 displays the plot of observed *vs*. calculated log($IC_{50}$).

**Table 4. Beta coefficients and t-test for significance of coefficients in Eq. 2**

| Var. | Beta | t(12) | p-level |
|---|---|---|---|
| $S_4^N(LUMO)*$ | -0.95 | -11.11 | <0.000001 |
| $S_{18}^E(HOMO-2)*$ | -0.34 | -4.01 | <0.002 |

**Table 5. Matrix of squared correlation coefficients for the variables in Eq. 2**

| | $S_4^N(LUMO)*$ | $S_{18}^E(HOMO-2)*$ |
|---|---|---|
| $S_4^N(LUMO)*$ | 1 | |
| $S_{18}^E(HOMO-2)*$ | 0.03 | 1 |

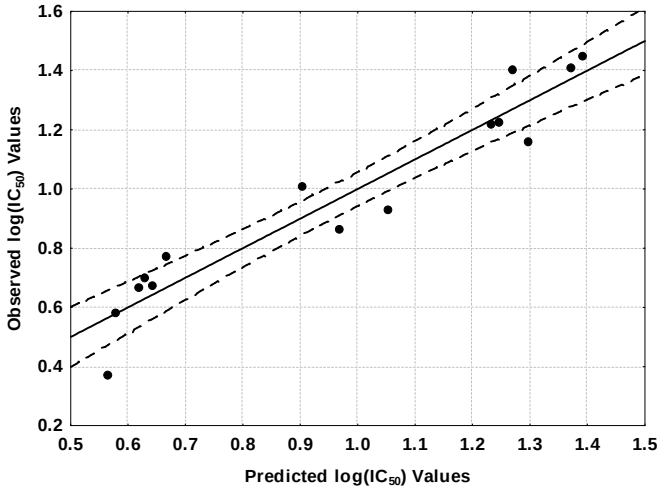


**Figure 4. Plot of predicted *vs*. observed log($IC_{50}$) values (Eq. 2). Dashed lines denote the 95% confidence interval**

The associated statistical parameters of Eq. 2 indicate that this equation is statistically significant and that the variation of the numerical values of a group of two local atomic reactivity indices of atoms of the common skeleton explains about 90% of the variation of log($IC_{50}$). Figure 4, spanning about 1 order of magnitude, shows that there is a good correlation of observed *versus* calculated values and that almost all points are inside the 95% confidence interval. This can be considered as an indirect evidence that the common skeleton hypothesis works relatively well for this set of molecules.

**Local Molecular Orbitals.**

Tables 6 and 7 show the local MO structure of atoms appearing in Eqs. 1 and 2 (see Fig. 2). Nomenclature: Molecule (HOMO) / (HOMO-2)* (HOMO-1)* (HOMO)* - (LUMO)* (LUMO+1)* (LUMO+2)*.

**Table 6. Local MO structure of atoms 4, 5 and 10**

| Mol. | Mol. | Atom 4 (C) | Atom 5 (C) | Atom 10 (C) |
|---|---|---|---|---|
| 1 (84) | 6a | 81π83π84π-85π86π87π | 82π83π84π-85π86π88π | 81π83π84π-85π87π89σ |
| 2 (84) | 6b | 82π83π84π-85π86π87π | 82π83π84π-85π86π88π | 78π81π84π-85π87π89σ |
| 3 (84) | 6c | 82π83π84π-85π86π87π | 82π83π84π-85π86π87π | 81π82π84π-85π86π87π |
| 4 (80) | 6d | 77π79π80π-81π82π83π | 78π79π80π-81π82π84π | 77π79π80π-81π83π85σ |
| 5 (80) | 6e | 78π79π80π-81π82π83π | 77π79π80π-82π84π87π | 74π77π80π-81π83π85σ |
| 6 (80) | 6f | 78π79π80π-81π82π83π | 77π78π79π-81π82π83π | 77π78π80π-81π83π85σ |
| 7 (87) | 6g | 85π86π87π-88π90π91π | 84π85π87π-88π90π91π | 84π86π87π-89π90π92π |
| 8 (87) | 6h | 85π86π87π-88π90π91π | 85π86π87π-88π90π92π | 85π86π87π-88π89π90π |
| 9 (87) | 6i | 84π86π87π-88π89π90π | 85σ86π87π-88π89π90π | 85σ86π87π-89π90π91π |
| 10 (80) | 6j | 78π79π80π-82π83π84π | 78π79π80π-82π83π84π | 77π79π80π-81π82π83π |
| 11 (80) | 6k | 78π79π80π-82π83π84π | 78π79π80π-82π83π84π | 77π78π80π-81π82π83π |
| 12 (80) | 6l | 78π79π80π-82π83π84π | 78π79π80π-82π83π84π | 75π77π80π-81π82π83π |
| 13 (84) | 6m | 81π83π84π-86π87π88π | 82π83π84π-86π87π88π | 81π83π84π-85π86π87π |
| 14 (84) | 6n | 81π82π84π-86π87π88π | 73π83π84π-86π88π90π | 81π83π84π-85π86π87π |
| 15 (84) | 6o | 81π82π84π-86π87π88π | 82π83π84π-86π87π88π | 81π83π84π-85π86π87π |

**Table 7. Local MO structure of atoms 11 and 18**

| Mol. | Mol. | Atom 11 (S) | Atom 18 (N) |
|---|---|---|---|
| 1 (84) | 6a | 77σ78π84π-85π86π87lp | 81π83π84π-85π86π87π |
| 2 (84) | 6b | 82π83π84π-85π86lp87lp | 82π83π84π-85π86π87π |
| 3 (84) | 6c | 80σ81π84π-85π86π87lp | 82π83π84π-85π86π87π |
| 4 (80) | 6d | 73σ74π80π-81π82π85lp | 77π79π80π-81π82π83π |
| 5 (80) | 6e | 78π79π80π-81π82lp83lp | 78π79π80π-81π82π83π |
| 6 (80) | 6f | 75σ77π80π-81π82π83lp | 78π79π80π-81π82π83π |
| 7 (87) | 6g | 85π86π87π-88π89π90π | 83σ86π87π-89π90π92π |
| 8 (87) | 6h | 85π86π87π-88π89π90π | 84σ86π87π-89π90π91π |
| 9 (87) | 6i | 85σ86π87π-88π89π91π | 83σ86π87π-89π90π91π |
| 10 (80) | 6j | 73σ74π80π-81π82π84lp | 78π79π80π-81π82π83π |
| 11 (80) | 6k | 77π79π80π-81π82lp83lp | 77π78π80π-81π82π83π |
| 12 (80) | 6l | 73σ75π80π-81π82π83lp | 78π79π80π-81π82π83π |
| 13 (84) | 6m | 79π83π84π-85π86π88lp | 80σ81π83π-85π86π87π |
| 14 (84) | 6n | 81π83π84π-85π86π88lp | 82π83π84π-85π86π87π |
| 15 (84) | 6o | 82π83π84π-85π86π87lp | 82π83π84π-85π86π87π |

## DISCUSSION

**Discussion of PDE3A inhibition.**

Table 3 shows that the importance of variables in Eq. 1 is $F_{11}(LUMO+2)^*$ > $F_{10}(LUMO+2)^*$ > $F_{11}(HOMO)^*$ >> $F_5(LUMO+2)^*$. A high inhibitory activity is associated with high numerical values for $F_{11}(LUMO+2)^*$, $F_{10}(LUMO+2)^*$ and $F_{11}(HOMO)^*$, and with low numerical values for $F_5(LUMO+2)^*$. Atom 5 is a carbon in ring A. $(LUMO)_5^*$, $(LUMO+1)_5^*$ and $(LUMO+2)_5^*$ have a π nature (Table 6). A high value for $F_5(LUMO+2)^*$ is associated with high inhibitory activity. Therefore, we suggest that atom 5 is interacting with an electron rich center through its first three lowest vacant MOs. The most probable interaction is of the π-π kind. Nevertheless, if we consider that Table 3 indicates that this LARI has a low statistical significance, we must take with care this suggestion. Atom 10 is a carbon in ring B. $(LUMO)_{10}^*$ and $(LUMO+1)_{10}^*$ have a π nature while $(LUMO+1)_{10}^*$ has σ or π natures (Table 6). A high value for $F_{10}(LUMO+2)^*$ is associated with high inhibitory activity. In the usual interpretation, when an occupied MO different from the HOMO* appears interacting it is accepted that the highest MOs also participate. The same holds for vacant MOs different from the LUMO*. For this case, the only way to give an account of the participation of π and σ MOs is by considering that atom 10 in more than one kind on interaction. Therefore, we suggest that atom 10 participates through π-π, π-σ and/or σ-σ interactions. Atom 11 is a sulphur in ring B. $F_{11}(LUMO+2)^*$ $F_{11}(HOMO)^*$ $(HOMO)_{11}^*$ is a π MO and $(LUMO+2)_{11}^*$ is a π or a lone pair MO (Table 7). A high inhibitory activity is associated with high numerical values for $F_{11}(HOMO)^*$ and $F_{11}(LUMO+2)^*$. Therefore, we suggest that atom 11 is engaged in a

π-π MO with one or more vacant MOs and through lone pair interactions with a negatively polarized π ring(s). All the suggestions are displayed in the partial 2D pharmacophore of Fig. 5.

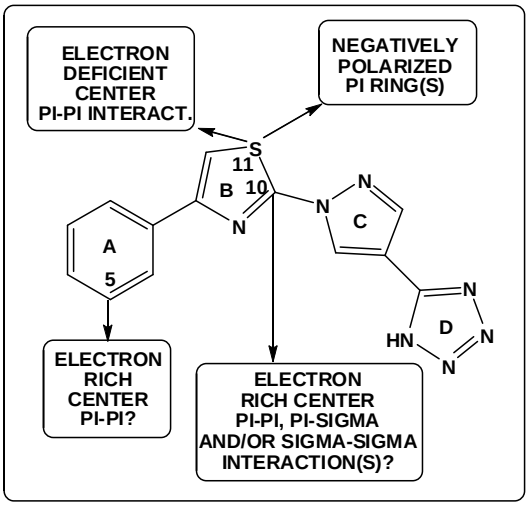


**Figure 5. Partial 2D pharmacophore for PDE3A inhibition**

**PDE3B INHIBITION**

Table 5 shows that the importance of variables in Eq. 2 is $S_4^N(LUMO)^* >> S_{18}^E(HOMO-2)^*$. A high inhibitory activity is associated with low (negative) numerical values for $S_{18}^E(HOMO-2)^*$. The case of $S_4^N(LUMO)^*$ will be discussed below. Atom 4 is a carbon in ring A. $(LUMO)_4^*$ has a π nature (Table 6). If $S_4^N(LUMO)^*$ is positive a high inhibitory activity is associated with high numerical values for this index. In the V-B-V analysis, this means that we need a more reactive MO to increase activity. This is obtained by shifting downwards the MO energy. Therefore, we suggest that atom 4 is interacting with an electron-rich center. Atom 18 is a nitrogen in ring D. $(HOMO-2)_{18}^*$ has σ or π natures while $(HOMO-1)_{18}^*$ and $(HOMO)_{18}^*$ have a π nature (Table 7). A high inhibitory activity is associated with small (negative) values for $S_{18}^E(HOMO-2)^*$. This suggests that a more active molecule should have the (HOMO-e2)* energy far below from the (HOMO-1)* or a zero electron population (i.e. this MO should not be localized on atom 18). Considering the nature of $(HOMO-1)_{18}^*$ and $(HOMO)_{18}^*$ we suggest that atom 18 is interacting with an electron deficient center. All the suggestions are displayed in the partial 2D pharmacophore of Fig. 6.

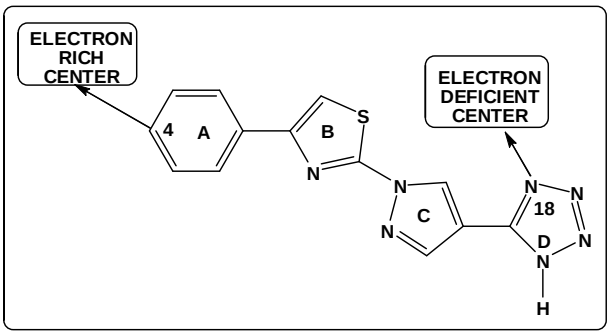


**Figure 6. Partial 2D pharmacophore for PDE3b inhibition**

Figure 5 shows that three reactivity indices belonging to ring B appear in Eq. 1. Figure 6 shows that one reactivity index belonging to ring D appears in Eq. 2. This can to be a direct effect of adding more molecular orbitals and/or to

the coplanarity of rings A-D. Both inhibitory processes are orbital-controlled as expected in highly selective biological structures.

In summary, we have obtained significant relationships between the electronic structure of a group of molecules and their PDE3A and PDE3B inhibitory capacity. The corresponding pharmacophores were built and they should provide information for future modifications of the common skeleton.

## REFERENCES

[1] TM Vinogradova, Y Lukyanenko, KV Tarasov, S Sirenko, AE Lyashkov, et al., *Biophys. J.*, **2016**, 110, 273a-274a.
[2] F Soler, F Fernández-Belda, J Pérez-Schindler, J Hernández-Cascales, *Eur. J. Pharmacol.*, **2015**, 765, 429-436.
[3] J Skogestad, *Biophys. J.*, **2015**, 108, 106a.
[4] M Houslay, *Nat. Gen.*, **2015**, 47, 562-563.
[5] DH Maurice, H Ke, F Ahmad, Y Wang, J Chung, et al., *Nat. Rev. Drug Discov.*, **2014**, 13, 290-314.
[6] Y-L Cai, Q Sun, X Huang, J-Z Jiang, M-H Zhang, et al., *Reg. Pept.*, **2013**, 180, 43-49.
[7] D Mika, J Leroy, G Vandecasteele, R Fischmeister, *J. Mol. Cell Cardiol.*, **2012**, 52, 323-329.
[8] M Movsesian, O Wever-Pinzon, F Vandeput, *Curr. Op. Pharmacol.*, **2011**, 11, 707-713.
[9] E Degerman, F Ahmad, YW Chung, E Guirguis, B Omar, et al., *Curr. Op. Pharmacol.*, **2011**, 11, 676-682.
[10] N Begum, W Shen, V Manganiello, *Curr. Op. Pharmacol.*, **2011**, 11, 725-729.
[11] A Galindo-Tovar, ML Vargas, AJ Kaumann, *Eur. J. Pharmacol.*, **2010**, 638, 99-107.
[12] H Dong, C Zitt, C Auriga, A Hatzelmann, PM Epstein, *Biochem. Pharmacol.*, **2010**, 79, 321-329.
[13] HA Walz, N Wierup, J Vikman, VC Manganiello, E Degerman, et al., *Cell. Sign.*, **2007**, 19, 1505-1513.
[14] J Leroy, A Abi-Gerges, W Richter, VO Nikolaev, S Engelhardt, et al., *J. Mol. Cell Cardiol.*, **2007**, 42, S49.
[15] E Zmuda-Trzebiatowska, A Oknianska, V Manganiello, E Degerman, *Cell. Sign.*, **2006**, 18, 382-390.
[16] R Nilsson, F Ahmad, K Swärd, U Andersson, M Weston, et al., *Cell. Sign.*, **2006**, 18, 1713-1721.
[17] B Ding, J-i Abe, H Wei, H Xu, W Che, et al., *Proc. Natl. Acad. Sci. USA*, **2005**, 102, 14771-14776.
[18] MA Movsesian, *J. Card. Fail.*, **2003**, 9, 475-480.
[19] T Aizawa, H Wei, J Miano, Ji Abe, B Berk, et al., *Atheroscl. Supp.*, **2003**, 4, 319.
[20] KS Murthy, H Zhou, *Gastroenterology*, **2001**, 120, A201.
[21] Y Shakur, LS Holst, TR Landstrom, M Movsesian, E Degerman, et al., "Regulation and function of the cyclic nucleotide phosphodiesterase (PDE3) gene family," in *Progress in Nucleic Acid Research and Molecular Biology*, vol. Volume 66, pp. 241-277, Academic Press, **2000**.
[22] A Hopitzan, H Himmelbauer, W Spevak, MJ Castanon, *Genomics*, **2000**, 66, 313-323.
[23] M Ahmad, PR Flatt, BL Furman, NJ Pyne, *Cell. Sign.*, **2000**, 12, 541-548.
[24] DM Essayan, *Biochem. Pharmacol.*, **1999**, 57, 965-973.
[25] M Conti, CB Andersen, FJ Richard, K Shitsukawa, A Tsafriri, *Mol. Cell. Endocrinol.*, **1998**, 145, 9-14.
[26] DC Bode, W Cumiskey, ED Pagani, PJ Silver, *J. Mol. Cell Cardiol.*, **1992**, 24, Supplement 3, S67.
[27] J Schneider, E Beck, *J. Mol. Cell Cardiol.*, **1991**, 23, Supplement 5, S43.
[28] FJR Rombouts, G Tresadern, P Buijnsters, X Langlois, F Tovar, et al., *ACS Med. Chem. Lett.*, **2015**, 6, 282-286.
[29] L-M Duan, H-Y Yu, Y-L Li, C-J Jia, *Biorg. Med. Chem.*, **2015**, 23, 6111-6117.
[30] P Buijnsters, M De Angelis, X Langlois, FJR Rombouts, W Sanderson, et al., *ACS Med. Chem. Lett.*, **2014**, 5, 1049-1053.
[31] K Ochiai, S Takita, A Kojima, T Eiraku, K Iwase, et al., *Bioorg. Med. Chem. Lett.*, **2013**, 23, 375-381.
[32] C Wang, TD Ashton, A Gustafson, ND Bland, SO Ochiana, et al., *Bioorg. Med. Chem. Lett.*, **2012**, 22, 2579-2581.
[33] M Ravinder, B Mahendar, S Mattapally, KV Hamsini, TN Reddy, et al., *Bioorg. Med. Chem. Lett.*, **2012**, 22, 6010-6015.
[34] SO Ochiana, A Gustafson, ND Bland, C Wang, MJ Russo, et al., *Bioorg. Med. Chem. Lett.*, **2012**, 22, 2582-2584.
[35] K Ochiai, S Takita, A Kojima, T Eiraku, N Ando, et al., *Bioorg. Med. Chem. Lett.*, **2012**, 22, 5833-5838.
[36] K Ochiai, S Takita, T Eiraku, A Kojima, K Iwase, et al., *Biorg. Med. Chem.*, **2012**, 20, 1644-1658.
[37] E Hu, RK Kunz, S Rumfelt, KL Andrews, C Li, et al., *Bioorg. Med. Chem. Lett.*, **2012**, 22, 6938-6942.
[38] H Sadeghian, *Clin. Biochem.*, **2011**, 44, S253-S254.
[39] K Ochiai, N Ando, K Iwase, T Kishi, K Fukuchi, et al., *Bioorg. Med. Chem. Lett.*, **2011**, 21, 5451-5456.

[40] RW Allcock, H Blakli, Z Jiang, KA Johnston, KM Morgan, et al., *Bioorg. Med. Chem. Lett.*, **2011**, 21, 3307-3312.
[41] M Nikpour, H Sadeghian, MR Saberi, RS Nick, SM Seyedi, et al., *Biorg. Med. Chem.*, **2010**, 18, 855-862.
[42] I Kim, JH Song, CM Park, JW Jeong, HR Kim, et al., *Bioorg. Med. Chem. Lett.*, **2010**, 20, 922-926.
[43] P Lacombe, N Chauret, D Claveau, S Day, D Deschênes, et al., *Bioorg. Med. Chem. Lett.*, **2009**, 19, 5266-5269.
[44] P Lacombe, D Deschênes, D Dubé, L Dubé, M Gallant, et al., *Bioorg. Med. Chem. Lett.*, **2006**, 16, 2608-2612.
[45] M Van der Mey, KM Bommelé, H Boss, A Hatzelmann, M Van Slingerland, et al., *J. Med. Chem.*, **2003**, 46, 2008-2016.
[46] SD Edmondson, A Mastracchio, J He, CC Chung, MJ Forrest, et al., *Bioorg. Med. Chem. Lett.*, **2003**, 13, 3983-3987.
[47] H Haning, U Niewöhner, T Schenke, M Es-Sayed, G Schmidt, et al., *Bioorg. Med. Chem. Lett.*, **2002**, 12, 865-868.
[48] G Nam, CM Yoon, E Kim, CK Rhee, JH Kim, et al., *Bioorg. Med. Chem. Lett.*, **2001**, 11, 611-614.
[49] MaI Crespo, J Gràcia, C Puig, A Vega, J Bou, et al., *Bioorg. Med. Chem. Lett.*, **2000**, 10, 2661-2664.
[50] G Buckley, N Cooper, HJ Dyke, F Galleway, L Gowers, et al., *Bioorg. Med. Chem. Lett.*, **2000**, 10, 2137-2140.
[51] JA Stafford, NL Valvano, PL Feldman, E Sloan Brawley, DJ Cowan, et al., *Bioorg. Med. Chem. Lett.*, **1995**, 5, 1977-1982.
[52] Note. The results presented here are obtained from what is now a routinary procedure. For this reason, we built a general model for the paper's structure. This model contains *standard* phrases for the presentation of the methods, calculations and results because they do not need to be rewritten repeatedly.
[53] JS Gómez-Jeria, *Int. J. Quant. Chem.*, **1983**, 23, 1969-1972.
[54] JS Gómez-Jeria, "Modeling the Drug-Receptor Interaction in Quantum Pharmacology," in *Molecules in Physics, Chemistry, and Biology*, J. Maruani Ed., vol. 4, pp. 215-231, Springer Netherlands, **1989**.
[55] JS Gómez-Jeria, M Ojeda-Vergara, *J. Chil. Chem. Soc.*, **2003**, 48, 119-124.
[56] JS Gómez-Jeria, *Elements of Molecular Electronic Pharmacology (in Spanish)*, Ediciones Sokar, Santiago de Chile, **2013**.
[57] JS Gómez-Jeria, *Canad. Chem. Trans.*, **2013**, 1, 25-55.
[58] JS Gómez-Jeria, *Res. J. Pharmac. Biol. Chem. Sci.*, **2016**, 7, 288-294.
[59] A Robles-Navarro, JS Gómez-Jeria, *Der Pharma Chem.*, **2016**, 8, 417-440.
[60] JS Gómez-Jeria, Í Orellana, *Der Pharma Chem.*, **2016**, 8, 476-487.
[61] JS Gómez-Jeria, C Moreno-Rojas, *Der Pharma Chem.*, **2016**, 8, 475-482.
[62] JS Gómez-Jeria, S Abarca-Martínez, *Der Pharma Chem.*, **2016**, 8, 507-526.
[63] HR Bravo, BE Weiss-López, J Valdebenito-Gamboa, JS Gómez-Jeria, *Res. J. Pharmac. Biol. Chem. Sci.*, **2016**, 7, 792-798.
[64] MJ Frisch, GW Trucks, HB Schlegel, GE Scuseria, MA Robb, et al., "G03 Rev. E.01," Gaussian, Pittsburgh, PA, USA, **2007**.
[65] JS Gómez-Jeria, "D-Cent-QSAR: A program to generate Local Atomic Reactivity Indices from Gaussian 03 log files. v. 1.0," Santiago, Chile, **2014**.
[66] JS Gómez-Jeria, *J. Chil. Chem. Soc.*, **2009**, 54, 482-485.
[67] Statsoft, "Statistica v. 8.0," 2300 East 14 th St. Tulsa, OK 74104, USA, **1984-2007**.